




Research Article

Restriction-site associated DNA sequencing data reveal a radiation of willow species (*Salix* L., Salicaceae) in the Hengduan Mountains and adjacent areasLi He^{1,2,3*} , Natascha Dorothea Wagner², and Elvira Hörandl²¹College of Forestry, Fujian Agriculture and Forestry University, Fuzhou 350002, China²Department of Systematics, Biodiversity and Evolution of Plants (with Herbarium), University of Goettingen, Göttingen, Germany³College of Biological Sciences and Technology, Beijing Forestry University, Beijing 100083, China

*Author for correspondence. E-mail: heli198724@163.com

Received 10 May 2019; Accepted 19 April 2020; Article first published online 24 April 2020

Abstract The Hengduan Mountains (HDM) in China are an important hotspot of plant diversity and endemism, and are considered to be a secondary diversification center for the woody plant genus *Salix* L. (Salicaceae). Here we aimed to reconstruct the spatiotemporal evolution of the *Salix Chamaetia-Vetrix* clade in the HDM and to test for the occurrence of a local radiation. We inferred phylogenetic relationships based on more than 34 000 restriction-site associated DNA loci from 27 species. Phylogenetic analyses recovered a well-resolved tree topology with two major clades, the Eurasian clade and the HDM clade, with a divergence time of ca. 23.9 Ma. Species in the HDM clade originated in the northern part of the range and adjacent areas, and then dispersed into the southern HDM, westwards to the Himalayas and eastwards to the Qinling Mountains. Niche modelling analyses reveal that range contractions occurred in the northern areas during the last glacial maximum, while southward expansions resulted in range overlaps. Reconstructions of character evolution related to plant height, inflorescence, and flower morphology suggest that adaptations to altitudinal distribution contributed to the diversification of the HDM willows. Our data support the occurrence of a radiation in the HDM within the *Salix Chamaetia-Vetrix* clade. Dispersal within the mountain system, and to adjacent regions, in addition to survival in glacial refugia shaped the biogeographical history of the clade, while adaptations of the HDM willows along an altitudinal gradient could be important ecological factors explaining the high species diversity of *Salix* in this area.

Key words: *Chamaetia-Vetrix* clade, divergence time, morphological adaptation, mountain radiation, phylogenomics, Qinghai–Tibetan Plateau.

1 Introduction

The Hengduan Mountains (HDM) are a temperate biodiversity hotspot located at the eastern end of the Himalaya and the south eastern margin of the Qinghai–Tibetan Plateau (QTP) (Li, 1987; Myers et al., 2000). The uplift of the HDM occurred mainly between the late Miocene and the late Pliocene (reviewed in Xing & Ree, 2017). The HDM are one of the ecologically most diverse areas in the QTP and adjacent regions; the HDM harbor more than 8559 species of vascular plants in approximately 1500 genera (Wu, 1988; Wang et al., 1993, 1994; Zhang et al., 2009). Approximately 32% of species are endemic to this region, making the HDM a significant global biodiversity hotspot (Myers et al., 2000).

Three areas of endemism have been identified within the HDM: northwest Yunnan, west Sichuan, and Sichuan–Gansu (López-Pujol et al., 2011). The 29°N latitudinal line is considered to be an important geographical division in the HDM, dividing the region into southern and northern subregions. The northern subregion includes west Sichuan and Sichuan–Gansu, and the southern subregion covers northwest Yunnan (Zhang et al., 2009).

Mountain biodiversity is driven by altitudinal gradients, climatic fluctuations, a high-relief terrain, and a diversity of ecological niches (Mosbrugger et al., 2018; Muellner-Riehl, 2019). Favre et al. (2015) discriminated four general scenarios for diversification in mountains systems: (i) ecological differentiation along altitudinal gradients; or

This is an open access article under the terms of the Creative Commons Attribution-NonCommercial-NoDerivs License, which permits use and distribution in any medium, provided the original work is properly cited, the use is non-commercial and no modifications or adaptations are made.

(ii) by colonization of new niches at higher altitudes; (iii) biogeographical differentiation through dispersal and local adaptation to higher altitudes; or (iv) after vicariance through geological processes. Disentangling these scenarios requires well resolved phylogenies and detailed reconstructions of biogeographical histories and ecological niches (Favre et al., 2015). Xing & Ree (2017) proposed that the HDM flora was mainly assembled by recent *in situ* diversification. Some studies reported that the uplift of the HDM and/or climatic oscillations in this region triggered plant radiations/diversification in several genera (Wen et al., 2014; Gao et al., 2015; Hou et al., 2016; Ebersbach et al., 2017; Xing & Ree, 2017). However, no study has so far tested whether radiations in the HDM followed a biogeographical north/south differentiation pattern, or ecological gradients. The role of vicariance versus dispersal is uncertain. Finally, Quaternary climatic oscillations influenced distribution patterns of plant species in the mountain systems of China (Qiu et al., 2011). Glaciation events during the last glacial maximum (LGM) could have caused extinction of species, and range fluctuations could have led to hybridization and polyploidization following secondary contact. Allopolyploidy can be considered to be a distinctive mechanism of species diversification and/or radiation in the HDM (Wen et al., 2014).

Radiations in mountain systems are usually thought to be connected to morphological adaptations to ecological conditions at higher altitudes (Körner, 2003). Adaptive radiations are characterized by key innovations that are driven by environmental factors and result in ecomorphological divergence (Simões et al., 2016). However, a pre-existing trait could also become advantageous under certain conditions (“exaptation” sensu Simões et al., 2016). Species in the QTP and adjacent areas (including HDM) with traits such as “glasshouse” leaves (e.g., *Rheum nobile* Hook. f. & Thomson), nodding flowers (*Cremanthodium* Benth.), downy bracts/leaves (*Eriophyton wallichii* Benth.), or cushion stature (e.g., *Salix* L. section *Lindleyanae*) are adapted to extreme environmental conditions (Fang et al., 1999; Zhang et al., 2010; Sun et al., 2014; Peng et al., 2015). Such adaptive morphological characters of these taxa could be key innovations and thus also a driver of diversification in HDM and adjacent areas (Wen et al., 2014; Muellner-Riehl et al., 2019).

In plants, reduction of plant size and protection of regenerative parts are the most obvious adaptations, leading to “alpine dwarfism” at highest elevations. The biomass of vegetative parts in higher altitudes is drastically reduced, whereas floral displays remain the same. Because pollination is often limited at high altitudes, improving pollinator attraction by various mechanisms (including increased flower size and nectar production) is an adaptation of high mountain plants, especially for obligate outcrossers (Körner, 2003; Fabbro & Körner, 2004). In mountain radiations, such traits are expected to differentiate according to altitudinal gradients.

The woody genus *Salix* L. includes ~450 species that are mostly distributed in the temperate, boreal, and arctic regions of the Northern Hemisphere (Fang et al., 1999; Skvortsov, 1999; Ohashi, 2006; Argus, 2010). This genus is considered a monophyletic group divided into two large clades based on molecular evidence: one comprising subgenus *Salix* and the other clade containing the *Chamaetia-Vetrix* subclade, *Chosenia*, and sections *Amygdalinae* and *Urbanianae* (Chen et al., 2010; Barkalov & Kozynenko, 2014; Percy et al., 2014; Lauron-Moreau

et al., 2015; Wu et al., 2015). Resolving relationships within the *Chamaetia-Vetrix* clade requires genomic data, but so far, only some European species have been analyzed (Wagner et al., 2018, 2019). The *Chamaetia-Vetrix* clade comprises approximately 385 species according to recent relevant floras and monographs, 226 of these occurring in China (Rechinger, 1993; Fang et al., 1999; Skvortsov, 1999; Ohashi, 2006; Argus, 2010). More than half of the 95 recorded species of the *Chamaetia-Vetrix* clade found in HDM are endemic or mainly distributed in this area. Although some of these species only occur in the northern subregion of HDM and its adjacent areas (e.g., *Salix magnifica* Hemsl., *S. phanera* C.K. Schneid., *S. oreinoma* C.K. Schneid., and *S. oritrepha* C.K. Schneid.), other species are found only in the southern region of HDM and adjacent areas, for example, *S. resecta* Diels, *S. cf. flabellaris* Andersson, and *S. psilostigma* Andersson (Fang et al., 1999). The relationships of these species to each other, and their phylogenetic position in the genus are so far unknown.

In the Himalaya–HDM and adjacent areas, the earliest *Salix* fossils are reported from the early and middle Miocene (17–15 Ma) (Tao, 2000; Spicer et al., 2003; Hui et al., 2011), younger than the fossil records of *Salix* in northeast China (Paleogene) (Tao, 2000), North America (Eocene) (Wolfe, 1987), and Europe (early Oligocene) (Collinson, 1992). Combined with a high rate of species diversity and endemism of *Salix* in the Himalaya–HDM region, several researchers suggested that this area might have acted as a secondary diversification center for the genus *Salix* (Fang & Zhao, 1981; Sun, 2002; Wang et al., 2017). However, this hypothesis lacks any comprehensive molecular phylogenetic support. Furthermore, little information is available on morphological and/or ecological diversification of *Salix* species in the HDM. The growth habit ranges from larger trees and shrubs to dwarf shrubs, size differences that might be adaptive along altitudinal gradients. As all willows are dioecious and both wind- and insect-pollinated, we expect that the mountain species would show adaptations to pollinator limitation or differences in the availability of biotic versus abiotic pollination vectors.

Here we use restriction-site associated DNA (RAD) sequencing data to reconstruct the phylogeny and spatiotemporal evolution of the *Chamaetia-Vetrix* clade, with a focus on the species of the HDM, testing for a putative radiation, and analyze whether diversification followed a north/south vicariance pattern or a pattern more indicative of dispersal within the HDM and adjacent regions. We also reconstruct the availability of climatic niches from global climatic data to obtain insights into the possible role of Quaternary climatic oscillations on species distribution. Finally, we analyze the evolution of selected adaptive morphological traits to obtain insights into the main factors that could have led to a putative radiation.

2 Material and Methods

2.1 Taxa sampling

In the HDM, 16 sections containing ~95 species of the *Chamaetia-Vetrix* clade are reported. Nine sections and more than half of the species are endemic or subendemic to this region. To cover the taxonomic species diversity in the HDM, we selected species to act as representatives of all nine endemic or subendemic sections in the HDM and adjacent

areas (i.e., QTP, the Himalayas, Qinling Mountains, and other parts of the southern China mainland; Tables S1, S2) (Fang et al., 1999). We also attempted to cover: (i) the morphological diversity of the group, sampling trees (e.g., *Salix phanera*), shrubs (e.g., *S. oritrepha*), and dwarf shrubs (e.g., *S. lindleyana* Wall. ex Andersson); and (ii) the distribution across altitudinal gradients (ranging from 570 m to 5200 m a.s.l.) inhabited by willows in the HDM and adjacent areas. Based on these initial considerations, we sampled 15 species of the *Salix Vetrix-Chamaetia* clade from the HDM and Nepal, each represented by one to four individuals, resulting in 46 accessions. Leaves of each sample were dried in silica gel. Voucher specimens collected for the present study are deposited in three herbaria: College of Forestry of Fujian Agriculture and Forestry University (FJFC), University of Goettingen (GOET), and University of Vienna (WU) (herbarium acronyms follow Thiers, 2020). Furthermore, 12 accessions of five widespread Chinese species, two of which (with six accessions) were published in Wagner et al. (2019), were included to cover five widely distributed non-endemic sections occurring in the HDM and adjacent areas. Finally, seven Eurasian *Salix* species (14 accessions) were published in Wagner et al. (2018) that represent the main Eurasian genetic clades; these were also included in this study to examine the overall position of the HDM species in *Salix* phylogeny. *Salix triandra* L. was used as an outgroup following Wagner et al. (2018). Source details of all 72 individuals representing 27 species are provided in Table S1.

2.2 Ploidy determination

The ploidy level of 47 samples was measured by flow cytometry, with a species of known ploidy (*S. caprea*; $2x = 2n = 38$) used as an external standard. The flow cytometry protocol of Suda & Trávníček (2006) was used for the dried leaf material. Silica gel-dried leaf materials ($\sim 1 \text{ cm}^2$ of each sample) were incubated for 80 min in 1 mL Otto I buffer (0.1 M citric acid, 0.5% Tween-20) at 4°C , and then chopped with a razor blade. After incubating for 10 min on ice, the homogenate was filtered through a $30 \mu\text{m}$ nylon mesh. The suspension was centrifuged at 12.5 g at 10°C for 5 min in a centrifuge (Heraeus Fresco 17 centrifuge; Thermo Eletron LED, Osterode, Germany); this was repeated two to three times for some samples, until a pellet of nuclei showed up. The supernatant was discarded, and the nuclei were resuspended with $200 \mu\text{L}$ Otto I buffer. Before the samples were analyzed, $800 \mu\text{L}$ Otto II (0.4 M $\text{Na}_2\text{HPO}_4 \cdot 12\text{H}_2\text{O}$) containing $4'$ -6-diamidino-2-phenylindole ($3 \mu\text{g mL}^{-1}$) was added and incubated for 30 min in the dark to stain the nuclei. DNA content measurements were done in a flow cytometer (CyFlow Space; Sysmex Partec, Münster, Germany), and FloMax version 2.0 (Sysmex Partec) was used to evaluate the histograms for each sample.

The ploidy level was calculated as: sample ploidy = reference ploidy \times mean position of the sample peak/mean position of reference peak. The quality of the measurements was evaluated by calculating coefficients of variation; the range of coefficients of variation varied between 5% and 11% (Table S1). Coefficients of variation values higher than 5% could be caused by the polyphenols of willow leaves and the use of dried samples (Doležel et al., 2007). To confirm our results, we compared our DNA content measurements with

previously known chromosome counts of *S. magnifica* and *S. psilostigma*. The results were congruent (i.e., $2x = 2n = 38$ for both species; Wilkinson, 1944; Fang et al., 1999).

2.3 DNA extraction and RAD sequencing

The total genomic DNA for all 52 samples was extracted from silica gel-dried leaves using the Qiagen DNeasy Plant Mini Kit (Qiagen, Valencia, CA, USA) following the manufacturer's instructions. DNA quality and concentration were verified and quantified using a NanoDrop 2000 (Thermo Fisher Scientific, CA, USA), and Qubit measurements in the Qubit 3.0 Fluorometer (Life Technologies Holdings, Singapore, Malaysia). The quantified DNA was sent to Floragenex (Portland, OR, USA). Restriction site-associated DNA sequencing library preparation and sequencing were undertaken as described in Wagner et al. (2018), following the method of Baird et al. (2008). The DNA was digested with *Pst*I, and sequenced on an Illumina HiSeq 2500 (Illumina, San Diego, CA, USA).

2.4 Restriction site-associated DNA sequencing data analysis

The raw sequence reads for all 52 samples were demultiplexed using IPYRAD version 0.6.15 (Eaton & Overcast, 2017). After the quality check by using FastQC version 0.10.1 (Andrews, 2010), the 52 demultiplexed FastQ files were analyzed in combination with the published 14 European and six Chinese accessions using the IPYRAD pipeline, with settings described in Wagner et al. (2018). Super-matrices for phylogenetic analyses were generated from three different thresholds of the minimum number of samples per locus, that is, m15 (loci shared by at least 15 samples), m25, and m40. Furthermore, for divergence time estimation, biogeographic analysis, and ancestral character evolution analyses, a reduced dataset was generated using one accession per species, resulting in 27 samples with an IPYRAD threshold of m15.

2.5 Phylogenetic inference of species relationships

Phylogenetic relationships were inferred by a maximum likelihood (ML) approach using RaxML version 8.2.4 (Stamatakis, 2014). Support values for each node were calculated using 100 rapid bootstrap replicates (-f a option) based on the GTR + GAMMA nucleotide substitution model.

Additionally, we used ExaBayes version 1.5 (Aberer et al., 2014) to undertake Bayesian analyses. Four independent runs were executed with three heated chains for 1 000 000 generations with sampling every 1000 generations. The first 20% of all samples were discarded as burn-in. Tracer version 1.7.1 (Rambaut et al., 2018) was used to check the effective sampling size values (>200) for all estimated parameters for convergence. The tools *postProcParam* and *sdsf* included in the ExaBayes package were used to calculate the potential scale reduction factor (close to 1) and the average standard deviation of split frequencies (less than 0.01). Finally, a consensus tree was generated by using the "consense" tool of the ExaBayes package. FigTree version 1.4.3 (Rambaut, 2014) was used to obtain all trees.

2.6 Divergence time estimation

To estimate divergence dates, we used BEAST version 1.7.5 (Drummond et al., 2012) with the reduced m15 dataset. The Bayesian uncorrelated log-normal strict molecular clock approach was applied using a GTR + Γ + I substitution model

with four rate categories and a Yule model prior on speciation. Given the thousands of concatenated RAD loci as input data, we assumed a common mutation rate across the genome (see Cavender-Bares et al., 2015). Posterior distributions of parameters were estimated using two independent Markov chain Monte Carlo analyses of 10 000 000 generations with a 10% burn-in. BEAST log files were analyzed with Tracer version 1.7.1 to assess convergence, and the combined tree files were used to generate a maximum clade credibility tree with median heights in TreeAnnotator version 1.7.5. The oldest reliable fossil determined as a member of subgenus *Vetrix* is known from Alaska and originated in the late Oligocene (Collinson, 1992). We calibrated the tree using this fossil, following Wu et al. (2015): the *Chamaetia-Vetrix* clade was assigned an exponential distribution prior with a mean of 1 and offset (hard bound constraint) of 23 Ma.

2.7 Ancestral character, altitudinal, and ancestral area reconstruction

We scored five morphological characters: (i) habit; (ii) relative time of flowering and emergence of leaves; (iii) catkin peduncle leaf type; (iv) staminate catkin shape; and (v) male flower abaxial nectary presence. We also scored altitudinal distribution. Data for all 27 included species were scored using floras (Rechinger, 1993; Fang et al., 1999; Ohashi, 2006; Argus, 2010), monographs (Martini & Paiero, 1988; Skvortsov, 1999; Argus, 2009; Hörandl et al., 2012), and through examination of herbarium material. Character state definitions and scorings are presented in Table S3. We used a parsimony unordered model to reconstruct ancestral states in

Mesquite 3.51 (Maddison & Maddison, 2018) based on the ML tree of the m15 reduced dataset.

The extant distribution of all 27 species, the subregions of HDM sensu Zhang et al. (2009), and the mountain systems were used to define biogeographic regions. Five regions were considered: A, eastern Himalaya, Khasi and Jaintia Hills, Naga Hills, and southeast QTP; B, north HDM, east QTP, and west Sichuan Basin; C, south HDM, Yungui Plateau, and south Sichuan Basin; D, Helan Mountains, Liupan Mountains, Qinling Mountains, Daba Mountains, Wu Mountains, Wuling Mountains, and east Sichuan Basin; and E, other parts of Asia, Europe, North Africa, and North America (Fig. 1). The distribution ranges (Table S4) of the species are based on data from the Chinese Virtual Herbarium (CVH, <http://www.cvh.ac.cn/>), Global Biodiversity Information Facility (GBIF, <https://www.gbif.org/>), examinations of specimens label information, and relevant published works (Wang et al., 1993; Fang et al., 1999; Skvortsov, 1999; Argus, 2010).

Ancestral areas were reconstructed using BioGeoBEARS (Matzke, 2014) in R version 3.5.1 (R Core Team, 2018). We tested three likelihood models, dispersal–extinction–cladogenesis (DEC), DIVALIKE, and BAYAREALIKE using the BioGeoBEARS package, using the Akaike information criteria to select the optimal model. We then calculated the probabilities of the ancestral states based on the dated tree, selecting the model that received the best Akaike information criteria score (Table S5).

2.8 Niche modelling

We obtained and selected 114 localities with precise records of HDM clade species from the CVH, GBIF, and specimens

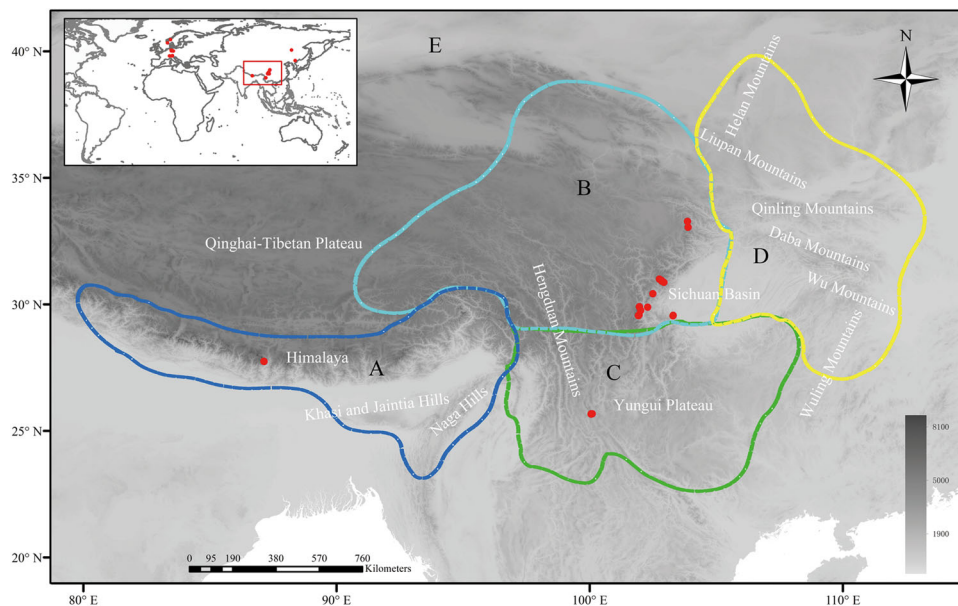


Fig. 1. Map of the studied area of the Qinghai–Tibetan Plateau (QTP), Himalayas, Hengduan Mountains (HDM), and adjacent mountain systems. Red dots indicate sample collection sites. Dotted colored lines show the biogeographic ranges for the ancestral area reconstruction. A, Eastern Himalayas, Khasi and Jaintia Hills, Naga Hills, and southeast QTP. B, North Hengduan Mountains, east QTP, and west Sichuan Basin. C, South Hengduan Mountains, Yungui Plateau, and south Sichuan Basin. D, Helan Mountains, Liupan Mountains, Qinling Mountains, Daba Mountains, Wu Mountains, Wuling Mountains, and east Sichuan Basin. E, Other parts of Asia, Europe, North Africa, and North America.

deposited in the Beijing Forestry University herbarium (BJFC, collected by the first author), and annotated records of the included samples (Table S6). The records are evenly distributed over the species from the HDM and adjacent regions. To ensure correct species identifications of these distribution sites, we re-examined all available specimens or digital images of specimens for each record.

Nineteen bioclimatic variables for the present day and LGM (CCSM), at a 2.5-arc-min resolution, were downloaded from the WorldClim database (<http://www.worldclim.org>) (Hijmans et al., 2005). We calculated Pearson correlation coefficients (R) for all pairs of bioclimatic variables, and used absolute value of R < 0.9 to remove highly correlated variables. Finally, we obtained 12 bioclimatic variables (Table S7). We used MAXENT version 3.4.1 (Phillips et al., 2018) to predict the current and LGM distributions of subclades I and II. The MAXENT analyses were carried out using 15 replicates each. The performance of each model prediction was tested by calculating the area under the receiver operating characteristic curve (AUC) (Phillips & Dudík, 2008). All distribution maps were visualized using ARCGIS 10.6.1 (ESRI, CA, USA).

3 Results

3.1 Ploidy determination

The ploidy level measuring and calculation of 47 individuals representing 16 species revealed that 12 species are diploid (Table S1). Diploid genomes were reported for the first time

for nine species (i.e., *Salix alfredii* Goerz ex Rehder & Kobuski, *S. atopantha* C.K. Schneid., *S. cf. flabellaris*, *S. dissa* C.K. Schneid., *S. hylonoma* C.K. Schneid., *S. oritrepha*, *S. phanera*, *S. resecta*, and *S. variegata* Franch.). *Salix lindleyana*, *S. ernestii* C.K. Schneid., and *S. oreinoma* were found to be tetraploid, and *S. opsimantha* C.K. Schneid. is hexaploid.

3.2 Restriction site-associated DNA sequencing

After quality filtering, the average number of 4.19 (+/-2.81) million reads per sample was used for subsequent analyses. An average of 105 960 (+/- 62 375) initial clusters per sample were generated. The average read depth was 52 reads per locus. After filtering, the IPYRAD pipeline recovered 33 626 (m15) to 19 492 (m40) RAD loci for the different thresholds. The concatenated alignment consisted of 120 822–193 694 parsimony informative sites. The reduced dataset (m15) of 27 accessions contained 34 945 RAD loci. Details for each dataset are listed in Table S8.

3.3 Phylogenetic analyses

Phylogenetic trees of the different RAD sequencing datasets (m15, m25, m40, and reduced m15) were constructed based on the ML and Bayesian inference methods, which recovered overall similar topologies using both methods (Figs. 2, S1, S2). Each species that included more than one specimen per species was recovered as monophyletic. Two major clades were resolved in the *Chamaetia-Vetrix* clade, which correspond to overall geographic distributions: an HDM clade (including

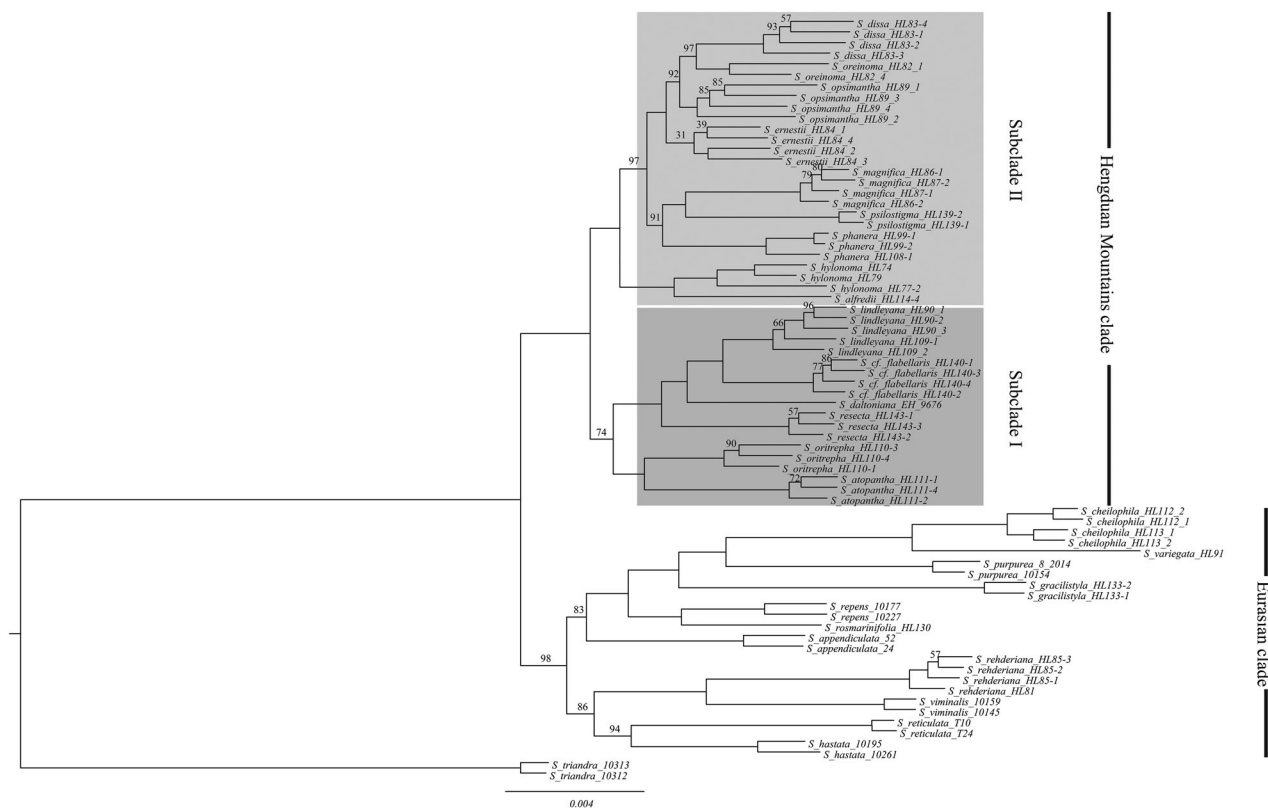


Fig. 2. Phylogeny inferred for 26 species (70 accessions) of the *Salix Chamaetia-Vetrix* clade and the outgroup *Salix triandra* (two accessions) based on maximum likelihood analyses of the m15 restriction site-associated DNA (RAD) sequencing dataset (33 626 RAD loci) using RAxML. Only bootstrap values less than 100% are indicated.

adjacent areas) and a Eurasian clade. The species of the HDM clade in turn form two subclades (I and II). Some sister-group relationships are consistent with monophyly of taxonomic sections (i.e., sect. *Sclerophyllae*, sect. *Lindleyanae*), whereas sect. *Psilostigmatae* was inferred to be non-monophyletic (Fig. 3). Almost all phylogenetic relationships received high bootstrap and posterior probability (Figs. 2, S1, S2).

3.4 Divergence time estimates

The topology derived from the BEAST analysis of the m15 reduced dataset is basically consistent with the ML trees and Bayesian trees of all datasets (Figs. 2, 4, S1, S2, S3). The estimate of the divergence time of the *Chamaetia-Vetrix* clade of 23.9 Ma (95% highest posterior density (HPD) 23–25.67 Ma) was based on fossil calibration (offset of 23 Ma) following Wu et al. (2015). The split between the Eurasian clade and HDM clade is estimated to be 23.9 Ma (95% HPD 23–25.67 Ma). The estimated crown age of subclade I is 14.73 Ma (95% HPD 14.09–15.85 Ma) and that of subclade II is 13.44 Ma (95% HPD 12.85–14.47 Ma). The youngest terminal nodes in subclade II occurred 7.92 Ma (95% HPD 7.5–8.54 Ma), and in subclade I 6.93 Ma (95% HPD 6.57–7.48 Ma, see Figs. 4, S3).

3.5 Biogeographical reconstructions

The DEC model was selected as the best-fitting model (Fig. 3). We infer that the origin of the HDM clade was most probably in the north HDM, east QTP, and west Sichuan Basin

(area B) followed by two independent predicted colonization events within subclades I and II into the south HDM, the Yungui Plateau, and the south Sichuan Basin (area C). In subclade I, colonization is predicted to have extended westwards to the eastern Himalayas, Khasi and Jaintia Hills, Naga Hills, and southeast QTP (area A). In subclade II, a dispersal route is predicted eastwards to the Helan Mountains, Liupan Mountains, Qinling Mountains, Daba Mountains, Wu Mountains, Wuling Mountains, and east Sichuan Basin (area D). The highest predicted colonization frequencies into area C from B were observed in the HDM clade.

3.6 Reconstructions of ancestral character states and altitude

The parsimony-based ancestral character state reconstructions of habit, staminate catkin shape, and elevation imply that plant height and male catkin length of the species within the HDM clade are associated with shifts in the altitudinal distribution. Overall, alpine species occurring at >3000 m a.s.l. have smaller plant size and shorter catkins compared to lowland species. The Eurasian clade consists of shrubs and trees mainly occurring at lower altitudes <3000 m. More specifically, within the HDM clade, we observed that tall shrubs or tree species in subclade II with slender male catkins occupy a lower altitudinal range of the HDM and adjacent areas, whereas smaller species at terminal nodes of

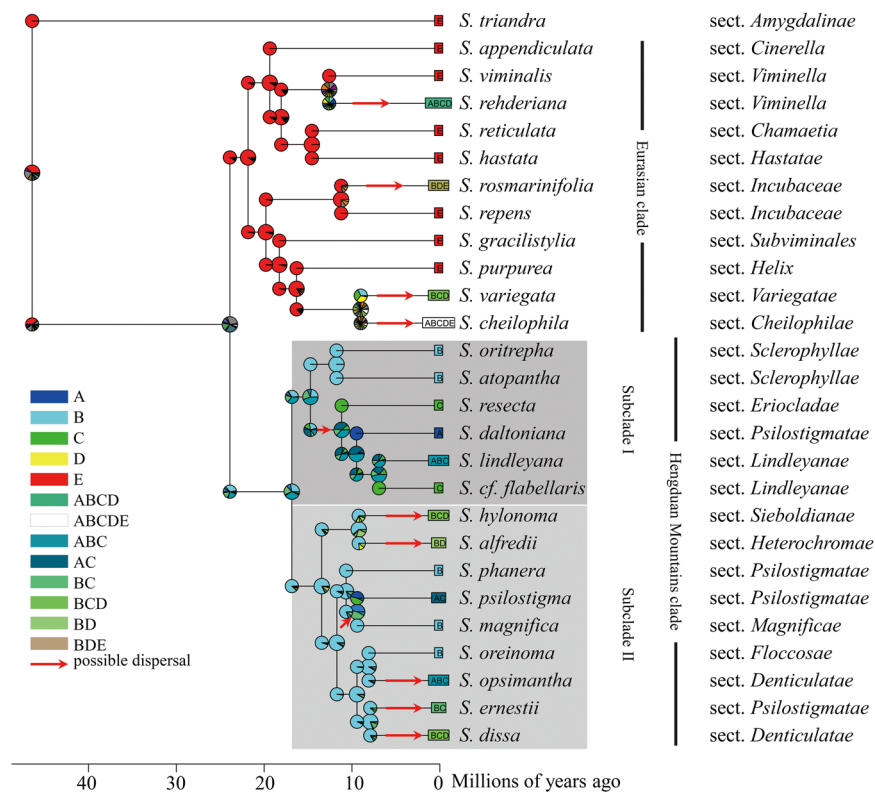


Fig. 3. Ancestral area reconstruction of the *Salix Chamaetia-Vetrix* clade based on the dispersal–extinction–cladogenesis likelihood method implemented in BioGeoBEARS. The topology and divergence times derived from the BEAST analyses of the m15-reduced data set based on fossil calibration (Fig. 4). Pie charts at the nodes represent the probability of regional occurrence. Red arrows show the possible dispersal events.

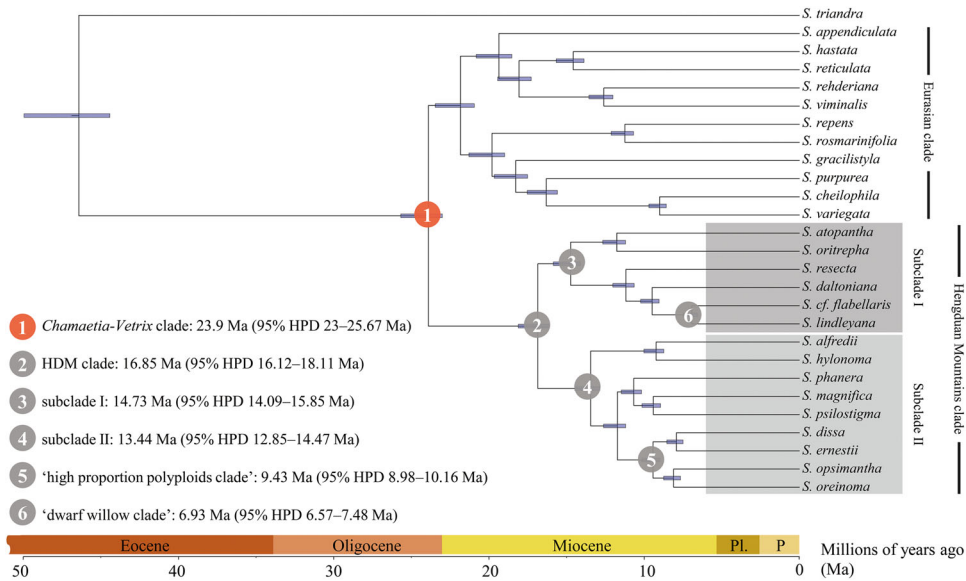


Fig. 4. Overview of the divergence times of the *Salix Chamaetia-Vetrix* clade based on the m15-reduced dataset. The date estimates for crown groups for clades 1–6 are given. The analysis was based on fossil calibration (23 Ma) following Wu et al. (2015). The node used for calibration is marked in red. Detailed divergence times for all nodes are given in Fig. S3. HPD, highest posterior density.

subclades I and II have stout catkins, and occur at higher altitudes (Figs. 5A, 5B, 6B).

The reconstruction of the remaining characters reveals that species of the HDM clade have foliate catkin peduncles and flower at the same time as leaves emerge. Additionally, they have an abaxial and an adaxial nectary in male flowers.

These characters are inferred to be plesiomorphic for the HDM clade and are otherwise shared with *S. reticulata* and the outgroup *S. triandra* (Fig. 6A). In contrast, the species of the Eurasian clade included here have precocious and bracteate catkins, and only one (adaxial) nectary as apomorphic states (Figs. 6A, S4).

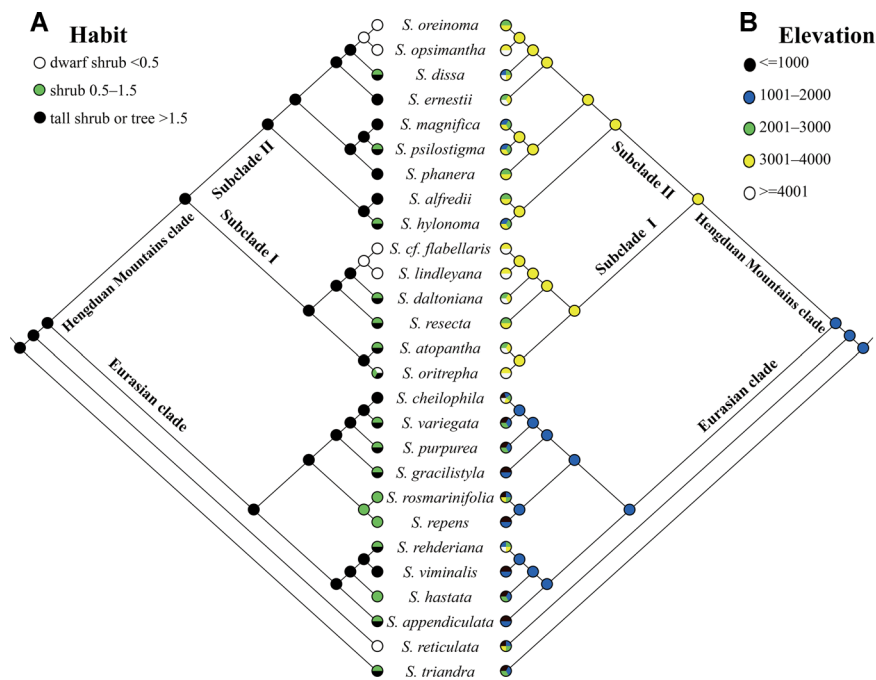


Fig. 5. Parsimony ancestral character-state reconstruction of (A) habit (height in m) and (B) elevation (a.s.l. in m) based on relationships implied by the RAxML tree of the m15 reduced dataset.

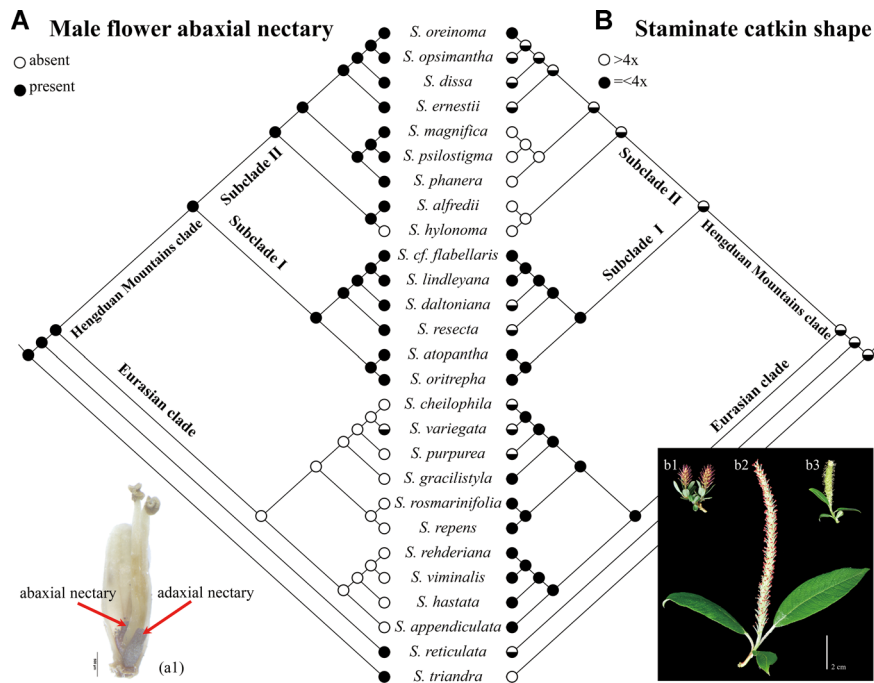


Fig. 6. Parsimony ancestral character state reconstruction of (A) male flower abaxial nectary presence and (B) staminate catkin shape (length (excluding peduncle)/width ratio) based on relationships implied by the RAxML tree of the m15 reduced dataset. Bottom left image: male flower with adaxial and abaxial nectary (a1, *Salix lindleyana*). Bottom right image: examples of stout staminate catkins (length excluding peduncle/width ratio = <4) of *S. lindleyana* (b1) and *S. atopantha* (b3) as well as of a slender catkin (length excluding peduncle/width ratio >4) of *S. phanera* (b2).

3.7 Niche modelling

The AUC values for the current potential climatically suitable areas of subclades I and II of the HDM clade were >0.96 and >0.92, respectively. This means the predictive models are substantially better than random expectation. The predicted present distributions of subclades I and II generally match the actual species distributions (Figs. 7A, 7B).

The niche modelling for the LGM for subclade I predicts range contractions for the western and northern parts of the potential species ranges in the eastern QTP and HDM (area B; Fig. 7C). However, we also predict slight expansions into the eastern Himalayas, Khasi and Jaintia Hills, Naga Hills (area A), and south HDM and Yungui Plateau (area C) (Fig. 7C).

For subclade II, the potential species range in the northeastern HDM is predicted to have contracted (area B) during the LGM. In contrast, expansions are predicted westwards to the eastern Himalayas, Khasi and Jaintia Hills, Naga Hills (area A), southwards to the southern HDM and Yungui Plateau (area C), and eastwards to the Qinling Mountains, Daba Mountains, and Wu Mountains (area D) (Fig. 7D).

4 Discussion

Here we used RAD sequencing data to investigate phylogenetic relationships of 27 species of the *Chamaetia-Vetrix* clade, with a specific focus on the spatiotemporal evolution of 15 representative species from the HDM. We also reconstructed the evolution of selected adaptive traits, and

undertook niche modelling to obtain insights into the possible role of climatic oscillations in relation to species distributions.

4.1 Phylogenomic analyses of the *Chamaetia-Vetrix* clade

Molecular studies to date for the *Chamaetia-Vetrix* clade of willows have either failed to resolve relationships within the *Chamaetia-Vetrix* clade (Chen et al., 2010; Barkalov & Kozyrenko, 2014; Percy et al., 2014; Lauron-Moreau et al., 2015; Wu et al., 2015), or included only a few species of this clade (Zhang et al., 2018b; Zhao et al., 2019). A well-resolved phylogeny of European species did not include, or included only one, *Salix* species from the HDM and adjacent areas (Wagner et al., 2018, 2019). Here, we present a well-resolved phylogeny of 27 *Salix* species and inferred two well-resolved clades: an HDM clade and a Eurasian clade (Figs. 2, 3, S1, S2). Our results support previous findings that RAD sequencing is a powerful tool for resolving phylogenetic relationships; the observed monophyly of the *Chamaetia-Vetrix* clade is also consistent with other molecular studies on genus *Salix* (Lauron-Moreau et al., 2015; Wu et al., 2015; Wagner et al., 2018, 2019).

We selected species in the Eurasian clade as representatives of the three main clades observed in Wagner et al. (2018). They were mainly included to test for the position of the samples from the HDM. Hence, our sampling is too small for broader taxonomic or biogeographical conclusions. However, five species collected from China are situated within the Eurasian clade. The widespread distribution of *S. cheilophila* C.K. Schneid., *S. gracilistyla* Miq., *S. rehderiana* C.K. Schneid., *S. variegata* L., and *S. rosmarinifolia* L. and their observed position in the inferred phylogeny implies that

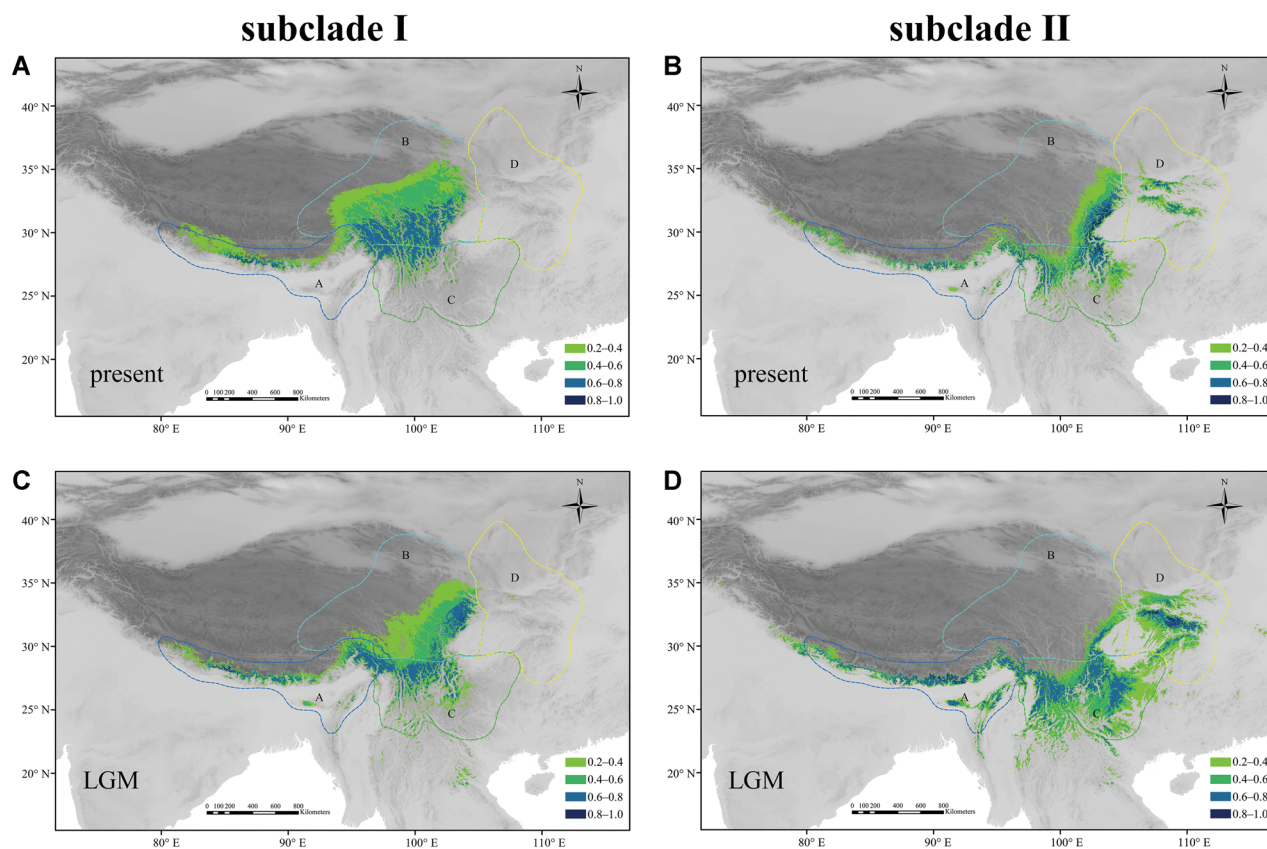


Fig. 7. Niche modelling analyses showing potential distributions as probabilities of occurrence for subclades I and II of the Hengduan Mountains clade of *Salix Chamaetia-Vetrix* clade. **A, B,** Under current conditions. **C, D,** At the last glacial maximum (LGM).

these species entered the HDM secondarily, rather than originating there (Figs. 2, 3).

The HDM clade consists of two subclades and is fully resolved. The 15 species of this clade represent nine sections that are endemic (or subendemic) to the HDM and adjacent areas and cover the species diversity in this region (Fig. 3; Table S2) (Wang et al., 1993; Fang et al., 1999). However, a comprehensive analysis based on a more complete sampling could reveal further colonization events of the HDM from Asia (Wu et al., 2015), but less likely from species of Europe (Wagner et al., 2019). Thus, we used this representative sampling to draw conclusions on the spatiotemporal evolution of the HDM willow species.

4.2 Spatiotemporal evolution of species of the *Chamaetia-Vetrix* clade in HDM

Almost 100 species of the *Chamaetia-Vetrix* clade occur in the HDM. More than half of these are endemic or mainly distributed in this area. Our phylogenomic results support the hypothesis that most species of the HDM represent a monophyletic lineage within the *Salix Chamaetia-Vetrix* clade (Figs. 2, 3, S1, S2) (Fang & Zhao, 1981; Sun, 2002; Wang et al., 2017). Our divergence time estimates imply that the HDM clade diverged from the Eurasian clade at 23.9 Ma (Fig. 4) in the late Oligocene. The observed age of the *Chamaetia-Vetrix* clade is consistent with the findings of Wu et al. (2015), but older than the estimated diversification

within extant *Salix* at ca. 20 Mya (13–28 Mya crown age) (Percy et al., 2014) and much older than diversification of observed haplotype groups within the genus made by the same authors. However, their phylogeny was based on two plastid markers (*matK* and *rbcl*) with a low number of informative sites, whereas our dating is based on more than 300 000 single nucleotide polymorphisms. The age is close to the divergence time of other alpine lineages in this region, for example, of *Rhodiola* L. (ca. 21.02 Ma) (Zhang et al., 2014). Additionally, the fossil record of *Salix* in the HDM and adjacent areas (17–15 Ma) is much younger than in other regions of the genus distribution area, which is consistent with our findings. We therefore predict that the willow radiation in the HDM is a rather recent and rapid radiation (Linder, 2008). Most plant radiations in the HDM are thought to have been driven by climatic oscillations throughout the last 7 Ma, as reviewed in Muellner-Riehl et al. (2019). The diversification of *Salix* observed here is much older and falls into the second rising period of the QTP (25–17 Ma; Shi et al., 1998). Our ancestral area reconstruction implies that the species of the HDM clade originated in the northern subregion of the HDM and adjacent areas. We predict the crown group diversification of the HDM clade to be approximately 17 Ma (Fig. 4), a time when the rise of the HDM had not yet started. The divergence of each of the two subclades (crown ages 13.4–14.7 Ma) also predated the uplift of the HDM between the late Miocene to late Pliocene (Xing & Ree, 2017). However, their crown ages coincide with the middle

Miocene climatic optimum (~17–14 Ma), in which there were warm conditions (Flower & Kennett, 1994; Miao et al., 2012) before worldwide cooling started (Miocene cooling).

Xing & Ree (2017) considered the uplift of the HDM to be an important driver for speciation, although they found an increased speciation rate around approximately 8 Ma, which is later than the observed start of diversification in our study. However, this might also reflect the fact that our sampling covered just the major lineages (sections), with only limited detail on later speciation events within these sections, which may well fall into this time period. In general, mountain uplift should result in fragmented habitats and the generation of newly established environments, thereby increasing biodiversity (Hoorn et al., 2013; Wen et al., 2014). A recent study on the QTP suggested that uplift had a higher impact on species diversity than climate fluctuations at this time period (Yu et al., 2018). However, the latter authors noted that there are strong interactions between these two factors. The fragmentation of mountains or “mountain relief” is an important factor in relation to species diversity and is specifically present in the HDM (Muellner-Riehl, 2019). Mountain relief causes strong elevation gradients with associated climatic gradients, and so leads to strong vertical zonation of vegetation (Nagy & Grabherr, 2009). Unlike other woody plants, willow species differentiate strongly in their habitat preferences along elevational gradients and cover many vegetation zones, as can be observed in the extant species of the European mountains (Hörandl et al., 2012; Wagner et al., 2018). In the HDM clade, a vertical differentiation appears in the terminal nodes of both subclades (Fig. 5). Hence, we assume that the uplift of the HDM had a stronger influence on the early diversification of willows in the HDM than climatic factors. Taken together, our study provides an example of a diversification pattern in the HDM that started before the strong climatic oscillations at the end of the Miocene (7 Mya), clearly predating the Quaternary (from ca. 2.6 Mya onwards), and more likely coinciding with the uplift of the HDM. After an initial diversification phase, the emergence of the rugged habitat of the HDM and associated gradients in elevation could have also triggered continued speciation in genus *Salix* in this area.

We do not observe a clear north/south pattern within the current HDM clade (Fig. 3). Given our representative sampling in terms of taxonomic and morphological diversity, we assume that additional taxa will fall into the given clades and will not alter our main predictions. Nevertheless, a more comprehensive taxon sampling would allow for fuller testing of the hypothesis of a north/south vicariance and independent radiations within the two subregions.

Subclade I diverged from subclade II at 16.85 Ma (Fig. 4). Within subclade I, we predicted a major dispersal event into the southern parts of the HDM (area C) and the eastern Himalayas (area A) at 14.73 Ma (Figs. 3, 4). Southward migration to more stable environments might be driven by global cooling (Spicer et al., 2003; Miao et al., 2012). The alpine dwarf willow clades (*S. lindleyana* and *S. cf. flabellaris*, *S. oreinoma*, and *S. opsimantha*) diverged at 6.93–8.1 Ma (Figs. 4, 5, S3), which might have been triggered by the uplift of the HDM in the late Miocene, as also suggested for *Lilium* L. and *Nomocharis* Franch. (Gao et al., 2015). Adaptation to niches at higher altitudes in subclade I is predicted to be one of the drivers of

speciation in mountain systems (Favre et al., 2015). Together with dispersal and the fragmented structure of the HDM, this could have led to the species radiation in this subclade.

For subclade II, our data revealed one migration event to the southern HDM approximately 9.4 Ma (Figs. 4, S3). However, this clade consists of more widely distributed species, which indicates that they might have spread eastwards and to lower altitudes (Figs. 3, 5B). Clade II comprises *Salix hylonoma* and *S. alfredii*, which could be a good example of species originating in the HDM and migrating along mountains ranges into central and northern China (“glacial out-of-Hengduan Mountains” hypothesis, Fan et al., 2013). Given our results and the examination of species distribution (Fang et al., 1999, this study), the migration route for *S. hylonoma* to central China was likely along the Yungui Plateau. The migration route for *S. alfredii* to central and northern China is predicted to be through the Qinling Mountains. Examples of migration routes out of QTP and adjacent areas into northern China were also described for other groups (Jia et al., 2012; Zhang et al., 2014), which took place in the Pliocene and Pleistocene, more recently than the divergence of the *S. hylonoma*–*S. alfredii* clade (divergence at ca. 9 Ma, Fig. S3). However, the overall pattern in willows of the HDM implies a scenario of dispersal combined with *in situ* ecological diversification, driven by the geomorphology and climate of the respective colonized area.

4.3 Influence of climatic oscillations and LGM

Climatic oscillations are regarded as important drivers of diversification in the QTP and the HDM (Wen et al., 2014) and in mountain systems in general (Favre et al., 2015; Muellner-Riehl et al., 2019). In contrast, our dated phylogeny suggests that the early diversification of the species of the HDM clade is much older than the Quaternary. Based on our sampling we cannot determine how the extant diversification of *Salix* in the HDM was affected by climatic oscillations during the Miocene/Pliocene. Quaternary climatic oscillations, however, were much stronger and connected to glaciations in the QTP–HDM mountain systems (Qiu et al., 2011; Zhang, 2012). Glaciations could have reduced net diversification by increasing extinction rates. Although we cannot calculate diversification rates with our taxon sampling, we can obtain insights into the possible effects of cold periods by considering what we know about LGM dynamics.

We undertook niche modelling analyses to trace the influence of the LGM on the range of the two subclades. We predict that LGM distributions of subclade I and II show an expansion to the southern parts of the HDM. The north–south orientation of major valleys (e.g., the Yangzi, the Mekong, and the Salween valleys) might have provided ice-free corridors for migration, avoiding the extinction of the affected *Salix* species during the glacial cycles, as suggested by Xing & Ree (2017). The HDM were not glaciated and likely acted as a refuge for many plants during glacial periods (reviewed in Qiu et al., 2011; Zhang et al., 2018a; Muellner-Riehl, 2019). The valleys could have also played a role for geographic isolation during a warm phase of climate oscillation, when the alpine *Salix* species colonized back to the northern parts of HDM, similar to the alpine plant *Marmoritis complanatum* (Dunn) A.L. Budantzev (Lamiaceae) (Luo et al., 2017).

Our results support the hypothesis that the southern lowlands of the Himalayas provided refugia for *Salix* and other plants throughout climatic oscillations and glaciation in the Quaternary (Qiu et al., 2011). Furthermore, they suggest that the Khasi and Jaintia Hills and Naga Hills connected the Himalayas with the HDM, and provided potential habitats for *Salix* species during the LGM. Overall, the high predicted number of refugia and migration routes likely preserved the species from extinction and might therefore in part explain the current high number of *Salix* species in the HDM.

The potential LGM distributions of the two subclades show more overlapping areas in the southern parts than in the present distribution (Fig. 7). Therefore, the glaciation could have also provided more chances for secondary contact of *Salix* species, potentially resulting in hybridization. Hybridization could affect phylogenetic reconstruction, potentially resulting in incorrect tree topologies (e.g., McDade, 1992; Linder & Rieseberg, 2004). Continued hybridization between non-sister taxa results in conflicting phylogenetic signals and decreasing bootstrap support (BS) at the backbone of the tree topology; hybridizing sister taxa will tend to show collapsed branches (e.g., Reeves & Richards, 2007). We cannot rule out that hybridization affects phylogenetic reconstruction in willows (Wu et al., 2015; Wagner et al., 2019). However, the tree topology of the HDM clade revealed 100% BS values at the backbone of the tree and for the clades of species, possibly supporting our assumption of a predominantly bifurcating tree topology. Homoploid hybridization and introgression after secondary contact of previously diverged species has been found in previously glaciated areas of the European Alps (Gramlich et al., 2016, 2018). Population genetic studies would be required to test for potential introgression and homoploid hybrid speciation in the HDM. In this regard, we detected some polyploid species in the HDM clade that might have originated from allopolyploidy. Allopolyploidy was considered to be another mechanism of the species diversification/radiations in the HDM (Wen et al., 2014). Chen et al. (2007) suggested that polyploidization played an important role in speciation in *Buddleja* L. (Buddlejaceae) in this area, also consistent with the findings of Ma et al. (2014) in *Bupleurum* L. (Apiaceae). However, our dating suggests that polyploidization events in the HDM happened long before the Quaternary and were contemporaneous with the shifts to higher altitudes (Fig. 4).

4.4 Possible adaptations of willows to higher altitudes

All willow species of the HDM clade can occur above the altitude of 3000 m (Fig. 5B). Their catkins mostly emerge together with leaves (coetaneous and serotinous) (Fig. S4A), and they usually have foliate catkins (Fig. S4B). This is consistent with Skvortsov (1999), who noted that the *Salix* species with coetaneous and serotinous catkins predominate in alpine zones. Young leaves at the base of the catkin cover the inflorescence at the early flowering stage, as with the bracts/leaves of “glasshouse” plants *Rheum nobile* that protect the young flowers from freezing damage (Skvortsov, 1999; Zhang et al., 2010). The species of the HDM clade share this trait, suggesting that the character might be important for them to survive cold periods and temperature extremes (Fang et al., 1999; Wen et al., 2014).

Protection of buds and young flowers is a general adaptive feature of alpine plants to avoid freezing damage (Körner, 2003).

The majority of the species of the HDM clade have male flowers that develop both an abaxial and an adaxial nectary (Fig. 6A), compared to the solitary adaxial nectary found in the Eurasian clade. Many *Salix* species are pollinated by both wind and insects (Karrenberg et al., 2002). However, Peeters & Totland (1999) found that predominantly insect-pollinated species produced more nectar. The abaxial nectary present in the species of the HDM clade may be an adaptation to higher altitudes to improve pollinator attraction (Figs. 5B, 6A). In turn, the elongated male catkins present in subclade II could be tentatively interpreted as an adaptation to a preferred wind-pollination syndrome at lower elevations, accompanied by increasing pollen quantity (Figs. 5B, 6B) (Karrenberg et al., 2002).

Mao et al. (2016) showed that the plant height of woody plants decreases significantly as altitude increases on the QTP (including parts of the HDM). Our results are consistent with their findings (Fig. 5). *Salix* species occur at different altitudes from deep valleys (1340 m, tall shrubs or tree willows like *S. psilostigma*) to alpine areas (up to 5200 m, e.g., the creeping willow *S. lindleyana*). This fits with a general finding of alpine dwarfism of plants at high altitudes (Körner, 2003). The high-alpine dwarf shrubs of sect. *Lindleyanae* are especially diverse in the alpine and high mountain areas of the HDM. Cushion stature shared by all species of this section was considered to reflect an adaptation to the QTP (Fang & Zhao, 1981), which is consistent with our results. The highly rugged terrain at high altitudes of the HDM along with the geographical isolation might have triggered bouts of speciation in this group.

Some of the characters we have discussed (abaxial nectary and foliate peduncles) are reconstructed as ancestral in the HDM clade (Figs. 6A, S4B), consistent with a hypothesis that the common ancestor of the HDM clade was already a mountain plant adapted to mid altitudes (see Fig. 5). These characters probably represent exaptations (sensu Simões et al., 2016) that have been advantageous in the HDM system, but did not diversify further. Plant height, and shape of catkins, however, differentiated at terminal lineages within the clade according to altitude, probably together with the emergence of a stronger relief during the uplift of the HDM ridges. Hence, both preadaptations and key innovations within the clade could have contributed to willow radiation.

Taken together, the observed differentiation of growth habit, catkin, and flower morphology according to different elevations supports a hypothesis that ecological diversification and adaptation might have been important drivers for the radiation of willows.

Acknowledgements

This study was financially supported by the German Research Foundation “Deutsche Forschungsgemeinschaft” (DFG project Ho 5462-7-1 to E.H.), by the National Natural Science Foundation of China (grant No. 31800466 to L.H.), and the Natural Science Foundation of Fujian Province of China (grant No. 2018J01613 to L.H.). L.H. was sponsored by the China

Scholarship Council for his research visit at the University of Goettingen (201707870015). We are indebted to Diego Hojsgaard, Piyal Karunaratne, Claudia Pätzold, and Marc Appelhans for their assistance in the early stages of the flow cytometry experiment, niche modelling analysis, Bayesian analysis, and biogeographical analysis, respectively. We are grateful to the curators and staff at the herbaria A, BJFC, FJFC, GOET, K, P, PE, SCFI, W, and WU for providing facilities and assistance or making high-quality specimen images available. We also thank Jun Zhao, Hai-lei Zheng, Wan-cheng Hou, Gong-ru Zhou for field assistance, Jian-quan Jin, and Kui-ling Zu for preparing plant materials, and Susanne Gramlich for sampling and DNA extractions.

References

- Aberer AJ, Kobert K, Stamatakis A. 2014. ExaBayes: Massively parallel Bayesian tree inference for the whole-genome era. *Molecular Biology and Evolution* 31: 2553–2556.
- Andrews S. 2010. FastQC: A Quality Control Tool for High Throughput Sequence Data [online]. Available from <http://www.bioinformatics.babraham.ac.uk/projects/fastqc>. [accessed 26 June 2018].
- Argus GW. 2009. *Salix* (willows) in the New World, a Guide to the Interactive Identification of Native and Naturalized Taxa Using Intkey (DELTA) [online]. Available from <https://www.albertaparks.ca/albertaparksca/science-research/interactive-salix-key/> [accessed 3 March 2018].
- Argus GW. 2010. *Salix*. In: Flora of North America Editorial Committee ed. *Flora of North America, Magnoliophyta: Salicaceae to Brassicaceae*. New York: Oxford University Press. 7: 23–51.
- Baird NA, Etter PD, Atwood TS, Currey MC, Shiver AL, Lewis ZA, Selker EU, Cresko WA, Johnson EA. 2008. Rapid SNP discovery and genetic mapping using sequenced RAD markers. *PLoS One* 3: e3376.
- Barkalov VY, Kozyrenko MM. 2014. Phylogenetic analysis of the Far Eastern *Salix* (Salicaceae) based on sequence data from chloroplast DNA regions and ITS of nuclear ribosomal DNA. *Botanica Pacifica* 3: 3–19.
- Cavender-Bares J, Gonzalez-Rodríguez A, Eaton DAR, Hipp AL, Beulke A, Manos PS. 2015. Phylogeny and biogeography of the American live oaks (*Quercus* subsection *Virentes*): A genomic and population genetics approach. *Molecular Ecology* 24: 3668–3687.
- Chen G, Sun WB, Sun H. 2007. Ploidy variation in *Buddleja* L. (Buddlejaceae) in the Sino-Himalayan region and its biogeographical implications. *Botanical Journal of the Linnean Society* 154: 305–312.
- Chen JH, Sun H, Wen J, Yang YP. 2010. Molecular phylogeny of *Salix* L. (Salicaceae) inferred from three chloroplast datasets and its systematic implications. *Taxon* 59: 29–37.
- Collinson ME. 1992. The early fossil history of Salicaceae: A brief review. *Proceedings of the Royal Society of Edinburgh, Section B: Biological Sciences* 98: 155–67.
- Doležel J, Greilhuber J, Suda J. 2007. Estimation of nuclear DNA content in plants using flow cytometry. *Nature Protocols* 2: 2233–2244.
- Drummond AJ, Suchard MA, Xie D, Rambaut A. 2012. Bayesian phylogenetics with BEAUti and the BEAST 1.7. *Molecular Biology and Evolution* 29: 1969–1973.
- Eaton DAR, Overcast I. 2017. Ipyrad: Interactive assembly and analysis of RADseq datasets [online]. Available from <http://ipyrad.readthedocs.io/> [accessed 20 June 2018].
- Ebersbach J, Schnitzler J, Favre A, Muellner-Riehl AN. 2017. Evolutionary radiations in the species-rich mountain genus *Saxifraga* L. *BMC Evolutionary Biology* 17: 1–13.
- Fabbro T, Körner C. 2004. Altitudinal differences in flower traits and reproductive allocation. *Flora* 199: 70–81.
- Fan DM, Yue JP, Nie ZL, Li ZM, Comes HP, Sun H. 2013. Phylogeography of *Sophora davidii* (Leguminosae) across the “Tanaka-Kaiyong Line,” an important phylogeographic boundary in Southwest China. *Molecular Ecology* 22: 4270–4288.
- Fang CF, Zhao SD, Skvortsov AK. 1999. Salicaceae. In: Wu ZY, Raven PH, Hong DY eds. *Flora of China*. Beijing: Science Press; St. Louis: Missouri Botanical Garden Press. 4: 139–274.
- Fang ZF, Zhao SD. 1981. On the origin and distribution of the genus *Salix* in Qinghai-Xizang Plateau. *Acta Phytotaxonomica Sinica* 19: 313–317.
- Favre A, Päckert M, Pauls SU, Jähnig SC, Uhl D, Michalak I, Muellner-Riehl AN. 2015. The role of the uplift of the Qinghai-Tibetan Plateau for the evolution of Tibetan biotas. *Biological Reviews of the Cambridge Philosophical Society* 90: 236–253.
- Flower BP, Kennett JP. 1994. The middle Miocene climatic transition: East Antarctic ice sheet development, deep ocean circulation and global carbon cycling. *Palaeogeography, Palaeoclimatology, Palaeoecology* 108: 537–555.
- Gao YD, Harris A, He XJ. 2015. Morphological and ecological divergence of *Lilium* and *Nomocharis* within the Hengduan Mountains and Qinghai-Tibetan Plateau may result from habitat specialization and hybridization. *BMC Evolutionary Biology* 15: 147.
- Gramlich S, Sagmeister P, Dullinger S, Hadacek F, Hörandl E. 2016. Evolution in situ: Hybrid origin and establishment of willows (*Salix* L.) on alpine glacier forefields. *Heredity* 116: 531–541.
- Gramlich S, Wagner ND, Hörandl E. 2018. RAD-seq reveals genetic structure of the F₂-generation of natural willow hybrids (*Salix* L.) and a great potential for interspecific introgression. *BMC Plant Biology* 18: 317.
- Hijmans RJ, Cameron SE, Parra JL, Jones PG, Jarvis A. 2005. Very high resolution interpolated climate surfaces for global land areas. *International Journal of Climatology* 25: 1965–1978.
- Hoorn C, Mosbrugger V, Mulch A, Antonelli A. 2013. Biodiversity from mountain building. *Nature Geoscience* 6: 154.
- Hörandl E, Florineth F, Hadacek F. 2012. *Weiden in Österreich und angrenzenden Gebieten (willows in Austria and adjacent regions)*. 2nd ed. Vienna: University of Agriculture.
- Hou Y, Nowak MD, Mirré V, Björå CS, Brochmann C, Popp M. 2016. RAD-seq data point to a northern origin of the arctic-alpine genus *Cassiope* (Ericaceae). *Molecular Phylogenetics and Evolution* 95: 152–160.
- Hui ZC, Li JJ, Xu QH, Song CH, Zhang J, Wu FL, Zhao ZJ. 2011. Miocene vegetation and climatic changes reconstructed from a sporopollen record of the Tianshui Basin, NE Tibetan Plateau. *Palaeogeography, Palaeoclimatology, Palaeoecology* 308: 373–382.
- Jia DR, Abbott RJ, Liu TL, Mao KS, Bartish IV, Liu JQ. 2012. Out of the Qinghai-Tibet Plateau: Evidence for the origin and dispersal of Eurasian temperate plants from a phylogeographic *Hippophae rhamnoides* (Elaeagnaceae). *New Phytologist* 194: 1123–1133.
- Karrenberg S, Kollmann J, Edwards PJ. 2002. Pollen vectors and inflorescence morphology in four species of *Salix*. *Plant Systematics and Evolution* 235: 181–188.

- Körner C. 2003. *Alpine plant life, functional plant ecology of high mountain systems*. 2nd ed. Berlin: Springer.
- Lauron-Moreau A, Pitre FE, Argus GW, Labrecque M, Brouillet L. 2015. Phylogenetic relationships of American Willows (*Salix* L., Salicaceae). *PLoS One* 10: e01211965.
- Li BY. 1987. On the boundaries of the Hengduan Mountains. *Journal of Mountain Research* 5: 74–82.
- Linder HP. 2008. Plant species radiations: Where, when, why? *Philosophical Transactions of the Royal Society B: Biological Sciences* 363: 3097–3105.
- Linder HP, Rieseberg LH. 2004. Reconstructing patterns of reticulate evolution in plants. *American Journal of Botany* 91: 1700–1708.
- López-Pujol J, Zhang FM, Sun HQ, Ying TS, Ge S. 2011. Centres of plant endemism in China: Places for survival or for speciation? *Journal of Biogeography* 38: 1267–1280.
- Luo D, Xu B, Li ZM, Sun H. 2017. The “Ward Line-Mekong-Salween Divide” is an important floristic boundary between the eastern Himalaya and Hengduan Mountains: Evidence from the phylogeographical structure of subnival herbs *Marmoritis complanatum* (Lamiaceae). *Botanical Journal of the Linnean Society* 185: 482–496.
- Ma XG, Zhao C, Wang BC, Liang QL, He XJ. 2014. Phylogenetic analyses and chromosome counts reveal multiple cryptic species in *Bupleurum commelynoideum* (Apiaceae). *Journal of Systematics and Evolution* 53: 104–116.
- Maddison WP, Maddison DR. 2018. Mesquite: A Modular System For Evolutionary Analysis. Version 3.51 [online]. Available from <http://www.mesquiteproject.org> [accessed 26 June 2018].
- Mao LF, Chen SB, Zhang JL, Zhou GS. 2016. Altitudinal patterns of maximum plant height on the Tibetan Plateau. *Journal of Plant Ecology* 11: 85–91.
- Martini F, Paiero P. 1988. *I Salici d'Italia: Guida al riconoscimento e all'utilizzazione pratica*. Trieste: Lint.
- Matzke NJ. 2014. Model selection in historical biogeography reveals that founder-event speciation is a crucial process in island clades. *Systematic Biology* 63: 951–970.
- McDade LA. 1992. Hybrids and phylogenetic systematics II: The impact of hybrids on cladistic analysis. *Evolution* 46: 1329–1346.
- Miao YF, Herrmann M, Wu F, Yan XL, Yang SL. 2012. What controlled mid-late Miocene long-term aridification in Central Asia? – Global cooling or Tibetan Plateau uplift: A review. *Earth-Science Reviews* 112: 155–172.
- Mosbrugger V, Favre A, Muellner-Riehl AN, Päckert M, Mulch A. 2018. Cenozoic evolution of geo-biodiversity in the Tibeto-Himalayan region. In: Hoorn C, Perrigio A, Antonelli A eds. *Mountains, Climate, and Biodiversity*. Chichester: Wiley-Blackwell. 429–448.
- Muellner-Riehl AN. 2019. Mountains as evolutionary arenas: Patterns, emerging approaches, paradigm shifts, and their implications for plant phylogeographic research in the Tibeto-Himalayan region. *Frontiers in Plant Science* 10: 195.
- Muellner-Riehl AN, Schnitzler J, Kissling WD, Mosbrugger V, Rijdsdijk KF, Seijmonsbergen AC, Versteegh H, Favre A. 2019. Origins of global mountain plant biodiversity: Testing the ‘mountain-geobiodiversity hypothesis’. *Journal of Biogeography* 46: 2826–2838.
- Myers N, Mittermeier RA, Mittermeier CG, da Fonseca GAB, Kent J. 2000. Biodiversity hotspots for conservation priorities. *Nature* 403: 853–858.
- Nagy L, Grabherr G. 2009. *The biology of alpine habitats*. Oxford: Oxford University Press.
- Ohashi H. 2006. Salicaceae. In: Iwatsuki K, Boufford DE, Ohba H eds. *Flora of Japan*. Tokyo: Kodansha. 11a: 7–25.
- Peeters L, Totland Ø. 1999. Wind to insect pollination ratios and floral traits in five alpine *Salix* species. *Canadian Journal of Botany* 77: 556–563.
- Peng DL, Niu Y, Song B, Chen JG, Li ZM, Yang Y, Sun H. 2015. Woolly and overlapping leaves dampen temperature fluctuations in reproductive organ of an alpine Himalayan forb. *Journal of Plant Ecology* 8: 159–165.
- Percy DM, Argus GW, Cronk QC, Fazekas AJ, Kesanakurti PR, Burgess KS, Husband BC, Newmaster SG, Barrett SCH, Graham SW. 2014. Understanding the spectacular failure of DNA barcoding in willows (*Salix*): Does this result from a trans-specific selective sweep? *Molecular Ecology* 23: 4737–4756.
- Phillips SJ, Dudík M. 2008. Modeling of species distribution with Maxent: New extensions and a comprehensive evaluation. *Ecography* 31: 161–175.
- Phillips SJ, Dudík M, Schapire RE. 2018. Maxent Software for Modeling Species Niches and Distributions. Version 3.4.1 [online]. Available from http://biodiversityinformatics.amnh.org/open_source/maxent/ [accessed 20 August 2018].
- Qiu YX, Fu CX, Comes HP. 2011. Plant molecular phylogeography in China and adjacent regions: Tracing the genetic imprints of Quaternary climate and environmental change in the world's most diverse temperate flora. *Molecular Phylogenetics and Evolution* 59: 225–244.
- R Core Team. 2018. R: A language and environment for statistical computing [online]. Vienna: R Foundation for Statistical Computing. Available from <https://www.R-project.org> [accessed 20 August 2018].
- Rambaut A. 2014. Figtree, A Graphical Viewer Of Phylogenetic Trees [online]. Available from <http://tree.bio.ed.ac.uk/software/figtree> [accessed 26 June 2018].
- Rambaut A, Drummond AJ, Xie D, Baele G, Suchard MA. 2018. Posterior summarization in Bayesian phylogenetics using Tracer 1.7. *Systematic Biology* 67: 901–904.
- Rechinger KH. 1993. *Salix*. In: Tutin TC, Burges NA, Chater AO, Edmondson JR, Heywood VH, Moore DM, Valentine DH, Walters SM, Webb DA eds. *Flora Europaea: Psilotaceae to Platanaceae*. 2 ed. Cambridge: Cambridge University Press. 1: 53–64. Revised by Akeroyed JR.
- Reeves PA, Richards CM. 2007. Distinguishing terminal monophyletic groups from reticulate taxa: Performance of phenetic, tree-based, and network procedures. *Systematic Biology* 56: 302–320.
- Shi YF, Tang MC, Ma YZ. 1998. The relation of second rising in Qinghai-Tibetan Plateau and Asian monsoon. *Science in China (D)* 28: 263–271.
- Simões M, Breitkreuz L, Alvarado M, Baca S, Cooper JC, Heins L, Herzog K, Lieberman BS. 2016. The evolving theory of evolutionary radiations. *Trends in Ecology and Evolution* 31: 27–34.
- Skvortsov AK. 1999. *Willows of Russia and adjacent countries*. Faculty of Mathematics and Natural Sciences Report Series, No. 39. Joensuu: University of Joensuu.
- Spicer RA, Harris NBW, Widdowson M, Herman AB, Guo S, Valdes PJ, Wolfe JA, Kelley SP. 2003. Constant elevation of southern Tibet over the past 15 million years. *Nature* 421: 622–624.
- Stamatakis A. 2014. RAxML version 8: A tool for phylogenetic analysis and post-analysis of large phylogenies. *Bioinformatics* 30: 1312–1313.

- Suda J, Trávníček P. 2006. Estimation of relative nuclear DNA content in dehydrated plant tissues by flow cytometry. *Current Protocols in Cytometry* 38: 1–14.
- Sun H. 2002. Evolution of Arctic-Tertiary flora in Himalayan-Hengduan mountains. *Acta Botanica Yunnanica* 24: 671–688.
- Sun H, Niu Y, Chen YS, Song B, Liu CQ, Peng DL, Chen JG, Yang Y. 2014. Survival and reproduction of plant species in the Qinghai–Tibet Plateau. *Journal of Systematics and Evolution* 52: 378–396.
- Tao JR. 2000. *The evolution of the Late-Cretaceous-Cenozoic flora of China*. Beijing: Science Press.
- Thiers B. 2020 [continuously updated]. Index Herbariorum: A global directory of public herbaria and associated staff [online]. New York Botanical Garden's Virtual Herbarium. Available from <http://sweetgum.nybg.org/science/ih/> [accessed 16 March 2020].
- Wagner ND, Gramlich S, Hörandl E. 2018. RAD sequencing resolved phylogenetic relationships in European shrub willows (*Salix* L. subg. *Chamaetia* and subg. *Vetrix*) and revealed multiple evolution of dwarf shrubs. *Ecology and Evolution* 8: 8243–8255.
- Wagner ND, He L, Hörandl E. 2019. Relationships and genome evolution of polyploid *Salix* species revealed by RAD sequencing data [online]. Available from <https://doi.org/10.1101/864504>.
- Wang QQ, Su XY, Shrestha N, Liu YP, Wang SY, Xu XT, Wang ZH. 2017. Historical factors shaped species diversity and composition of *Salix* in eastern Asia. *Scientific Reports* 7: 42038.
- Wang WT, Wu SG, Lang KY, Li PQ, Pu FT, Chen SK. 1993. *Vascular plants of the Hengduan Mountains: Pteridophyta, Gymnospermae, Dicotyledoneae (Saururacea to Cornaceae)*. Beijing: Beijing Science and Technology Press.
- Wang WT, Wu SG, Lang KY, Li PQ, Pu FT, Chen SK. 1994. *Vascular plants of the Hengduan Mountains: Dicotyledoneae (Diapensiaceae to Asteraceae) to Monocotyledoneae (Typhaceae to Orchidaceae)*. Beijing: Beijing Science and Technology Press.
- Wen J, Zhang JQ, Nie ZL, Zhong Y, Sun H. 2014. Evolutionary diversifications of plants on the Qinghai-Tibetan Plateau. *Frontiers in Genetics* 5: 4.
- Wilkinson J. 1944. The cytology of *Salix* in relation to its taxonomy. *Annals of Botany* 8: 269–284.
- Wolfe JA. 1987. Late Cretaceous-Cenozoic history of deciduousness and the terminal Cretaceous event. *Paleobiology* 13: 215–226.
- Wu J, Nyman T, Wang DC, Argus GW, Yang YP, Chen JH. 2015. Phylogeny of *Salix* subgenus *Salix* s.l. (Salicaceae): Delimitation, biogeography, and reticulate evolution. *BMC Evolutionary Biology* 15: 31.
- Wu ZY. 1988. Hengduan Mountain flora and her significance. *Journal Japanese Botany* 63: 297–311.
- Xing Y, Ree RH. 2017. Uplift-driven diversification in the Hengduan Mountains, a temperate biodiversity hotspot. *Proceedings of the National Academy of Sciences USA* 114: E3444–E3451.
- Yu HB, Deane DC, Sui XH, Fang SQ, Chu CJ, Liu Y, He FL. 2018. Testing multiple hypotheses for the high endemic plant diversity of the Tibetan Plateau. *Global Ecology and Biogeography* 2018: 1–14.
- Zhang DC, Boufford DE, Ree RH, Sun H. 2009. The 29°N latitudinal line: An important division in the Hengduan Mountains, a biodiversity hotspot in southwest China. *Nordic Journal of Botany* 27: 405–412.
- Zhang DY, Liu BB, Zhao CM, Lu X, Wan DS, Ma F, Chen LT, Liu JQ. 2010. Ecological functions and differentially expressed transcripts of transgenic bracts in an alpine ‘glasshouse’ plant *Rheum nobile* (Polygonaceae). *Planta* 231: 1505–1511.
- Zhang JQ, Meng SY, Allen GA, Wen J, Rao GY. 2014. Rapid radiation and dispersal out of the Qinghai-Tibetan Plateau of an alpine plant lineage *Rhodiola* (Crassulaceae). *Molecular Phylogenetics and Evolution* 77: 147–158.
- Zhang JQ, Zhong DL, Song WJ, Zhu RW, Sun WY. 2018a. Climate is not all: Evidence from phylogeography of *Rhodiola fastigiata* (Crassulaceae) and comparison to its closest relatives. *Frontiers in Plant Science* 9: 462.
- Zhang L, Xi ZX, Wang MC, Guo XY, Ma T. 2018b. Plastome phylogeny and lineage diversification of Salicaceae with focus on poplars and willows. *Ecology and Evolution* 7: 7817–7823.
- Zhang LS. 2012. *Palaeogeography of China: The formation of China's natural environment*. Beijing: Science Press.
- Zhao YJ, Liu XY, Guo R, Hu KR, Cao Y, Dai F. 2019. Comparative genomics and transcriptomics analysis reveals evolution patterns of selection in the *Salix* phylogeny. *BMC Genomics* 20: 253.

Supplementary Material

The following supplementary material is available online for this article at <http://onlinelibrary.wiley.com/doi/10.1111/jse.12593/supinfo>:

Fig. S1. Phylogeny inferred for 26 species of the *Salix Chamaetia-Vetrix* clade and the outgroup *S. triandra* based on maximum likelihood analyses of the m15-reduced dataset (A), m25 (B), and m40 (C) RAD sequencing data sets using RAXML. Only bootstrap values less than 100% are shown beside branches.

Fig. S2. Phylogeny inferred for 26 species of the *Chamaetia-Vetrix* clade *Salix*, and *S. triandra*, based on Bayesian analyses of the m15-reduced dataset (A), m15 (B), m25 (C), and m40 (D) RAD sequencing data set using ExaBayes. Posterior probability (PP) values are given above branches.

Fig. S3. Estimate of divergence times of the *Chamaetia-Vetrix* clade of *Salix* based on the m15-reduced data set. Date estimates were based on fossil calibration (23 Ma) following Wu et al. (2015). The 95% highest posterior densities (HPDs) are given above branches. Numbers in nodes represent their estimated ages. Posterior probability (PP) value of each clade is 1 and not shown on the topology.

Fig. S4. Parsimony ancestral state reconstruction of relative time of flowering and emergence of leaves (a) and catkin peduncle leaf type (b) based on relationships revealed by the RAXML tree of the m15 reduced dataset.

Table S1. Details of plant materials used in this study, the samples with gray background were from Wagner et al. (2018) and Wagner et al. (2019).

Table S2. The 16 sections of *Chamaetia-Vetrix* clade that occur in HDM.

Table S3. Data matrix of morphological characters and altitude distribution for the 27 *Salix* species and relevant states.

Table S4. Data matrix of the distribution areas in this study for the 27 *Salix* species.

Table S5. Comparison of the fitting of different models of ancestral geographic region analyses and model specific estimates for the different parameters [d = dispersal, e = extinction].

Table S6. The information of the localities of subclade I and II used in the niche modelling analyses.

Table S7. The 12 bioclimatic variables obtained for the niche modelling analyses in subclade I and II.

Table S8. The statistics for four different parameters of the ipyrad analyses of 27 species.

Data S1. Sequence data are available from the Dryad Digital Repository: <https://doi.org/10.5061/dryad.3ffbg79fd>